http://www.diva-portal.org

Postprint

This is the accepted version of a paper published in *Microelectronics and reliability*. This paper has been peer-reviewed but does not include the final publisher proof-corrections or journal pagination.

Citation for the original published paper (version of record):

Tegehall, P-E., Wetter, G. (2015)
Impact of laminate cracks under solder pads on the fatigue lives of ball grid array solder joints
Microelectronics and reliability, 55(11): 2354-2370
https://doi.org/10.1016/j.microrel.2015.07.014

Access to the published version may require subscription.

N.B. When citing this work, cite the original published paper.

Permanent link to this version:
http://urn.kb.se/resolve?urn=urn:nbn:se:ri:diva-13298

Impact of Laminate Cracks under Solder Pads on the Fatigue Lives of Ball Grid Array Solder Joints

P.-E. Tegehall*, G. Wetter

Swerea IVF, Box 104, SE-431 22 Mölndal, Sweden

* Corresponding author
E-mail address: per-erik.tegehall@swerea.se
Tel.: +46 31 7066148

Abstract

This paper reports how the solder joint fatigue lives of three types of lead free plastic BGA components were affected by cracks formed in the printed PCB laminate during a thermal cycling test. The investigation showed that cracks were formed in the laminate for all three tested components. For one of the components having a large chip with solder joints located under the chip, very large cracks were formed in the PCB laminate beneath some solder pads.

For lead-free solder joints to BGA components consisting of near eutectic solders based on tin, silver and copper, a large fraction of the solder joints may consist of one single tin grain. Due to anisotropy of tin grains, each solder joint to a BGA component will experience a unique stress condition which will make laminate cracking more likely under certain solder joints.

The laminate cracks increased the flexibility of the joints and thereby improved the fatigue lives of the solder joints. Therefore, an estimation of the fatigue lives of solder joints to BGA components based on the results from a thermal cycling test may lead to an overestimation of the fatigue lives if products will be exposed to smaller temperature changes in the field than in the test.

If cracks are not formed in the PCB laminate, or if the extent of cracking is small, single-grained solder joints can be expected to result in a high spread in failure distribution with some quite early failures.

Keywords: solder joint reliability, laminate cracking, lead-free soldering, anisotropy of tin grains, BGA components.

1 Introduction

Comparisons of the thermo-mechanical fatigue lives of SnPb and lead-free solder joints of Ball Grid Array (BGA) components have shown that lead-free solder joints generally have longer fatigue lives than SnPb solder joints in low-stress conditions [1]. Under such conditions, the fatigue lives of SnAgCu solder joints with 3.0 wt-% Ag and 0.5 wt-% Cu (SAC305) may be 50-100% longer compared to SnPb solder joints [2-4]. However, in high-stress conditions, the difference in fatigue lives are smaller or even reversed [1].

The stress on solder joints in a thermal cycling test are affected by a large number of factors. Two of the most important are the temperature range (delta T) used in the test and the mismatch of the coefficients of thermal expansion (CTE) between a component and the PCB. However, plastic IC components are not homogenous and the CTE varies for different parts of the components. For a BGA, the CTE is determined by the CTE of several different materials and, therefore, may vary significantly for various parts of the component. The build-up of a typical plastic BGA is shown in Fig. 1. For this type of BGA, the CTE is mainly determined by the CTEs of the laminate (substrate) to which the chip is attached, the die attach material, the chip and the moulding compound. Due to the large difference in CTE between the chip and the other materials, the area of the BGA laminate located under the chip will have a much lower CTE compared to the area outside the chip, and also compared to a polymeric printed circuit board (PCB). The effective CTE of this area will be affected not only by the CTE of the various materials but also by the thicknesses of the materials (laminate, die attach material and chip) and by the elastic modulus of these materials and then especially that of the die attach material. Hence, solder joints to a BGA component located under the chip will experience a high CTE mismatch between the component and the PCB resulting in a high-stress condition in a thermal cycling test.

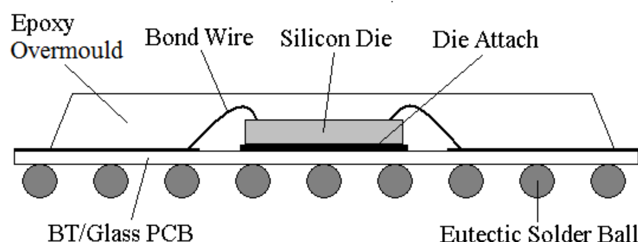

Fig. 1. Schematic cross-section of a plastic BGA of OMPAC type (over moulded plastic pad array carrier).

During the last 10 years, component manufacturers have gradually changed to new moulding compounds and today most IC components are probably manufactured using these new compounds [5]. There are several reasons for this change. One of the main reasons is to decrease the amount of water absorbed when the components are exposed to ambient conditions prior to soldering in order to avoid high internal vapour pressure during soldering. This has been achieved in the new moulding compounds by increasing both the level of inorganic fillers and the degree of cross-linking of the polymer. Thereby, it has also been possible to pass flame retardancy requirements without addition of flame retardant compounds. The new moulding compounds are therefore promoted as green moulding compounds. The high content of inorganic fillers gives them a very low CTE of 6-10 ppm/°C. That can be compared with sintered alumina used in ceramic components which has a CTE of about 7 ppm/°C. Thus, for BGAs produced using these new low-CTE moulding compounds, also the part of the BGA outside the chip area will have a rather low CTE. Simulations done

by imec have shown that this may decrease the fatigue life of the solder joints with up to 85% [5, 6].

The stress a solder joint will be exposed to in a thermal cycling test will also be affected by the elastic modulus and the glass transition temperature (T_g) for polymeric materials in the component and the PCB. A lower elastic modulus (more elastic material) will decrease the stress on the solder joints. Since the CTE of polymeric materials usually increases considerably above T_g, cycling to temperatures above T_g will result in a larger CTE mismatch. On the other hand, the elastic modulus is usually considerably lower at temperatures above T_g. Therefore, increasing the upper temperature in a thermal cycling test above T_g may actually result in lower stress on the solder joints.

In the case of lead-free soldering, there is also another important factor affecting the stress on the solder joints. In contrast to SnPb solder joints, which consist of a large number of tin-rich and lead-rich grains, SAC solder joints to BGAs often consist of only one or a few tin grains [7-12]. Exceptions are solder joints with small solder volume [9, 12] and lead-free solders based on tin and silver with no copper [11]. In both these latter cases, the solder joints will have interlaced Sn grain morphology with many grains.

Tin grains are highly anisotropic. That is, the properties differ in various crystallographic directions. The CTE of pure tin grains at ambient conditions varies between approximately 15 ppm/°C (a- and b-axes) and 30 ppm/°C (c-axis), and the elastic modulus varies between approximately 22 and 69 GPa [7, 11, 13]. Furthermore, both CTE and elastic modulus are highly dependent on temperature. At 125°C, the CTE various between 20 and 40 ppm/°C and the elastic modulus between 15 and 60 GPa [11].

Single-grained solder joints with the c-axis parallel to the PCB surface have been shown to be much more prone to fatigue during thermal cycling compared to solder joints with the c-axis perpendicular to the PCB surface, at least for BGA solder joints exposed to comparatively low strain [7, 11, 14]. For BGA solder joints exposed to very high strain, such as BGAs with 0.4-0.5 mm pitch, the orientation of the tin grains has less influence on the fatigue of the solder joints [14].

Thus, the number of tin grains and the orientation of the grains in a SAC solder joint will have a large impact on the resulting stress levels. Several studies have shown that the orientation of the tin grains has a nearly random distribution [7, 8, 15]. This means that there may be a large difference in stress levels even for two neighbouring solder joints. Consequently, the solder joints to fail first in an array of SAC solder joints to a BGA, which is not fine pitch, may be more or less randomly distributed as have been shown in several studies [8, 16, 17]. These solder joints may be far away from the point of maximum shear stress for a corresponding BGA with SnPb solder joints. This is not observed for BGAs with Sn/Ag solder joints [16], probably due to the fact that Sn/Ag solder joints have a multi-grained microstructure.

High stress on the solder joints during temperature changes caused by the CTE mismatch may not only result in fatigue of the solder joints, it may also cause formation of cracks in the PCB and BGA laminates. The cracks are usually formed near and under the solder pads and are often called pad craters since they leave a crater in the laminate if the pads are ripped off. This type of crack is mainly associated with very high strain rates caused by bending, drops or vibration, but cracks in the laminates may also be caused by thermal cycling or during cool-down in a soldering process [18-23]. An increase of delta T during thermal cycling has been shown to increase the likelihood for pad cratering [22].

This paper reports on how the increase of the CTE mismatch between components, solder and PCB due to lead-free soldering may affect the failure mechanism in a thermal cycling test due

to cracks formed in the PCB and BGA laminates. The results are from a larger study investigating the impact of lead-free soldering on the reliability of solder joints to components prone to fatigue in automotive applications. In this study the extensive laminate cracking came as a surprise. That is, the test had not been designed to study this phenomenon.

2 Experimental work

2.1 Manufacture of test boards

The test board used for the evaluations was a four-layer board with a thickness of 1.6 mm, and with copper planes in the two inner layers. The circuitry on the top-layer, where all interconnections were done, is shown in Fig. 2.

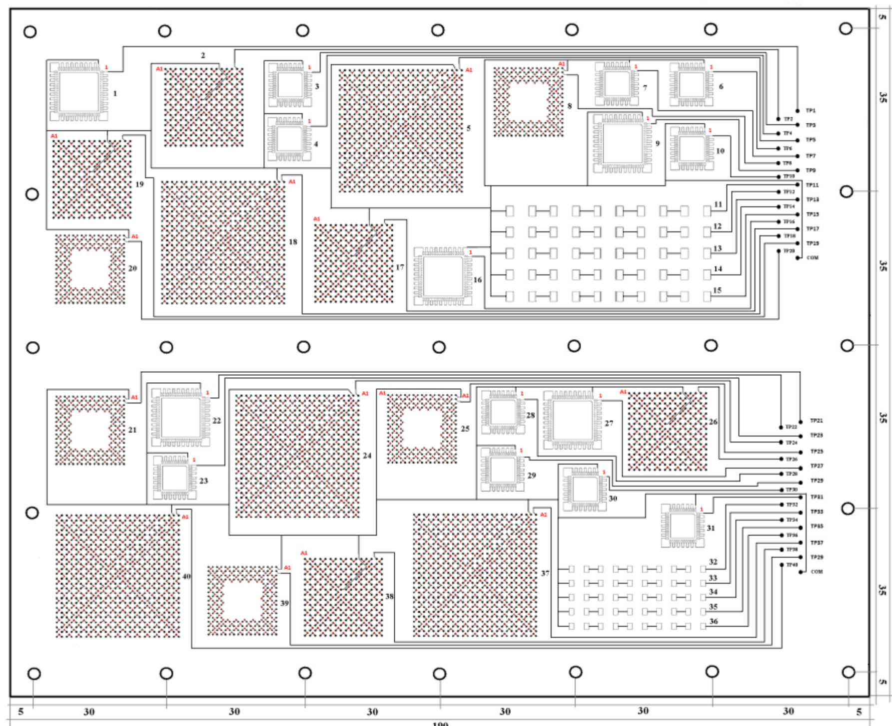

Fig. 2. Layout of the top layer of the test board

The test board laminate was a commonly used high performance FR-4 laminate with a T_g of 180°C conforming to IPC-4101C/21/24/26/98/99/101/126. According to the laminate manufacturer, the laminate had CTE values of 14 and 17 ppm/°C in the x- and y-directions, respectively.

The test boards were produced with four different surface finishes: SnPb HASL (hot air solder levelling), SN100C HASL, ENIG (Electroless Nickel/Immersion Gold) and ImAg (Immersion Silver). A solder mask was applied to the test boards. The SnPb HASL boards were used for manufacturing of reference boards with SnPb solder joints.

The following types of components were soldered to the test boards: BGA208, BGA256, BGA676, QFN48, QFN72 and ceramic resistors of sizes 1206 and 2512. The BGAs were supplied both with SnPb and SAC305 solder balls. Five components of each type could be mounted on the test board except the ceramic resistors for which 25 components of each type could be mounted. Two test boards were produced with each combination of solder finish and solder to be tested. Only some of the results for the BGAs will be reported here.

The BGA208 component was a Thin Core Ball Grid Array (CTBGA) whereas the two other BGAs were plastic BGAs (PBGA). All were of the OMPAC-type. Data for the tested BGAs are given in Table 1.

Table 1 Data for the BGA components used.

Component	Pitch	Body size	Ball matrix	Ball alignment	Chip size
BGA208	0.8 mm	15 mm	17x17	Perimeter, 4 rows	11.5 mm
BGA256	1.0 mm	17 mm	16x16	Full array	5 mm
BGA676	1.0 mm	27 mm	26x26	Full array	17 mm

All BGAs had daisy-chain interconnections. When analysed with energy dispersive X-ray spectroscopy (EDX), no bromine or antimony could be detected in the moulding compounds indicating the absence of brominated flame retardants. Thus, it is likely that all BGAs had been produced using low CTE moulding compounds.

The daisy chain interconnections on the PCB for the BGA208 are shown Fig. 3. The connections between the solder pads on the PCB are all passing through an annular ring to a via. Thereby, by measuring the resistance between two vias next to each other in the daisy chain from the opposite side of the test board, solder joints with increased resistance could be identified to pairs of solder joints in the daisy chain. The daisy chains for the BGA256 and BGA676 components were designed similarly.

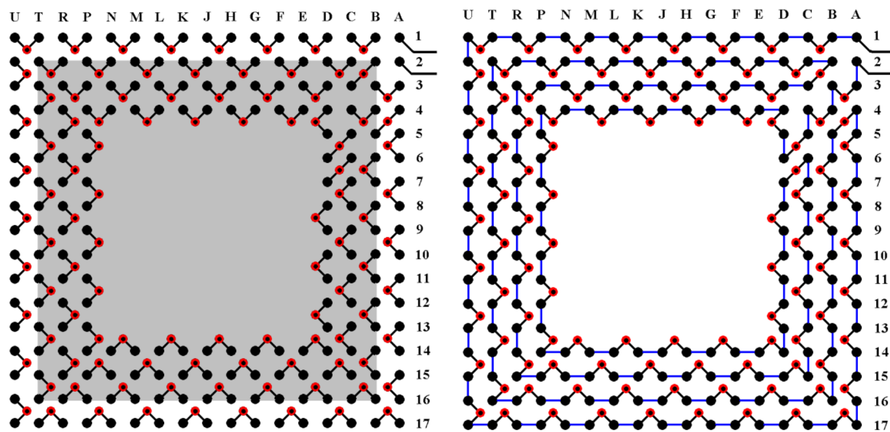

Fig. 3. Daisy-chain interconnections for the BGA208 on the board (left image) and the complete daisy chain (right image). Larger (black) dots represent solder pads and smaller (red) dots vias. The grey square shows the size of the chip in the component.

The types of solder pad definition and the sizes of the solder pads on the PCB for the BGAs are presented in Table 2. In order to optimise solder joint fatigue, it is important to have a pad design that provides a balanced stress on the solder joints. Since all BGAs had solder mask defined (SMD) pads, this was also chosen for the BGA256 and BGA676 components which both had 1.0 mm pitch. The reason non-solder mask defined (NSMD) pads were chosen for the BGA208 component is that the line-routing space between the pads becomes too small for components with 0.8 mm pitch if SMD pads are used. In order to still get a balanced stress on the solder joints, the area of the solder pads was reduced with 15% compared to the solderable area on the BGA208 component according to recommendations by Altera [24].

Table 2 Types and sizes of solder pads on the PCB for the various BGA components.

Component	Pitch	Type of solder pad	Diameter of solder pad	Diameter of solder mask opening
BGA208	0.80 mm	NSMD	0.30 mm	0.50 mm
BGA256	1.00 mm	SMD	0.65 mm	0.45 mm
BGA676	1.00 mm	SMD	0.65 mm	0.45 mm

The test boards were soldered by a company producing automotive electronics using their regular production lines for SnPb and lead-free soldering. The test matrix is given in Table 3. Soldering was done at two different occasions. The boards with HASL finishes were soldered first and the boards with the other finishes were soldered five months later. An exception was the boards with SN100C finish that were soldered with SN100C solder paste (Board ID 3e) which were also soldered five months later. The SnPb reference boards were soldered using a Sn62Pb36Ag2 solder paste whereas the lead-free boards were soldered using either a SAC305 or a SN100C solder paste. For the lead-free soldering, the peak temperature was about 240°C, the time above liquidus about 60 s and the cooling rate about 2°C/s in the temperature range 220-100 °C. At both production occasions, the solder paste print was defective for the BGA208 component. Some solder paste remained in some stencil openings but solder paste was printed on all solder pads. No cleaning was performed after soldering.

Table 3 Test matrix used for the thermal cycling test.

Board ID	PCB finish	Solder paste	Testing
2a	SN100C HASL	SAC305	Thermal cycling
2b	SnPb HASL	SnPb	
3a	SN100C HASL	SAC305	Ageing + Thermal cycling
3b	SnPb HASL	SnPb	
3c[a]	ENIG	SAC305	
3d[a]	ImAg	SAC305	
3e[a]	SN100C HASL	SN100C	
3f[a]	ENIG	SN100C	
3g[a]	ImAg	SN100C	

[a] Soldered five months after the other boards.

2.2 Thermal cycling

Most of the assembled boards were aged for 500 h at 125°C prior to the thermal cycling test (see Table 3). Thermal cycling was performed between -40°C and +125°C. The dwell times were 10 min at -40°C and 20 min at +125°C, and the temperature change rate was 5°C/min both when heating and cooling. That makes a total cycle time of 96 min. The boards that were soldered first were cycled for 5167 cycles (about 11 months) whereas the boards soldered five months later were cycled for 4030 cycles.

2.3 Failure detection

High-speed event detectors were used during the thermal cycling test for monitoring the daisy chain resistance *in situ*. The event detectors could detect ultra-short resistance spikes or open circuits provided that they were at least 1 μs long. An open circuit in this case was defined as a total daisy chain resistance above 100 Ω. A failure was defined when ten consecutive events were detected within 10% of current life of the test.

2.4 Resistance measurements of the daisy chains

After the thermal cycling test had been finished, pairs of solder joints with increased resistance or open solder joints where localised by measuring the resistance between via holes from the backside of the test boards. This was done for three to four components with each tested combination of solder finish and solder composition.

2.5 Cross-sectioning of samples

Cross-sectioning of samples included careful cutting out of samples from the test board using a high-speed diamond saw, followed by moulding in room temperature hardening epoxy in a low-vacuum step. The cross-sectioned samples were prepared through successive grinding and polishing down to the areas of interest. All cross-sections were done in parallel to an edge of the cross-sectioned components.

A fluorescent agent was added to the moulding resin in order to facilitate the detection of very fine cracks when inspected in UV-light. This is especially useful for detection of cracks in the PCB and BGA laminates since both the material surrounding a crack and the moulding compound then consist of epoxy.

2.6 Dye penetrant analysis

The extent of cracking in the solder joints to some of the components was analysed using dye penetrant analysis, also called “dye and pry” test. The samples were also in this case cut out from the test boards using a high-speed diamond saw. They were then cleaned for 60 min in Zestron FA at 50°C followed by drying at 125°C for 60 min. The cleaning was done in order to enable the dye to more easily penetrate fractures by removing all flux residues. The samples were then immersed in Dykem Red Steel layout fluid in a small tray and the tray was placed into a vacuum chamber. The pressure in the vacuum chamber was decreased to about 0.2 bar and was then increased to 1 bar. This was repeated two times.

After the samples had been removed from the tray, excess dye was allowed to drain off. They were then allowed to dry at ambient conditions for a few hours before they were finally dried at 100°C for 60 min. The components were then mechanically removed by repeatedly flexing the boards until the components easily could be pried off.

3 Results

3.1 Lead-free versus SnPb solder joints on HASL PCBs

The results from the failure detection using the event detector for the thermally cycled boards were evaluated using two parameter Weibull plots. From the Weibull plots, the characteristic life (eta) and the slope parameter (beta) were calculated. Eta is the time at which 63.2 % of the population is expected to fail whereas beta shows how the failure rate develops in time. The larger the beta value, the narrower is the failure distribution. In addition to eta and beta values, the correlation coefficient (r^2) and the number of samples starting/surviving (n/s) the test are given in the table on the graphs.

The results from the thermal cycling of lead-free boards (SAC305 solder joints to SN100C HASL) and SnPb reference boards (SnPb solder joints to SnPb HASL) with no aging prior to the test are presented in Fig. 4, whereas the results for the boards that were aged prior to the test are presented in Fig. 5. With possibly one exception for one of the lead-free BGA208 components on a non-aged board, the high beta values indicate that the imperfect solder paste

print for this component type did not affect the fatigue lives of the solder joints. The early failure for the lead-free BGA208 on the non-aged board, however, may be due to an effect of the anisotropy of tin grains and not defective solder paste print as will be discussed in the Discussion section.

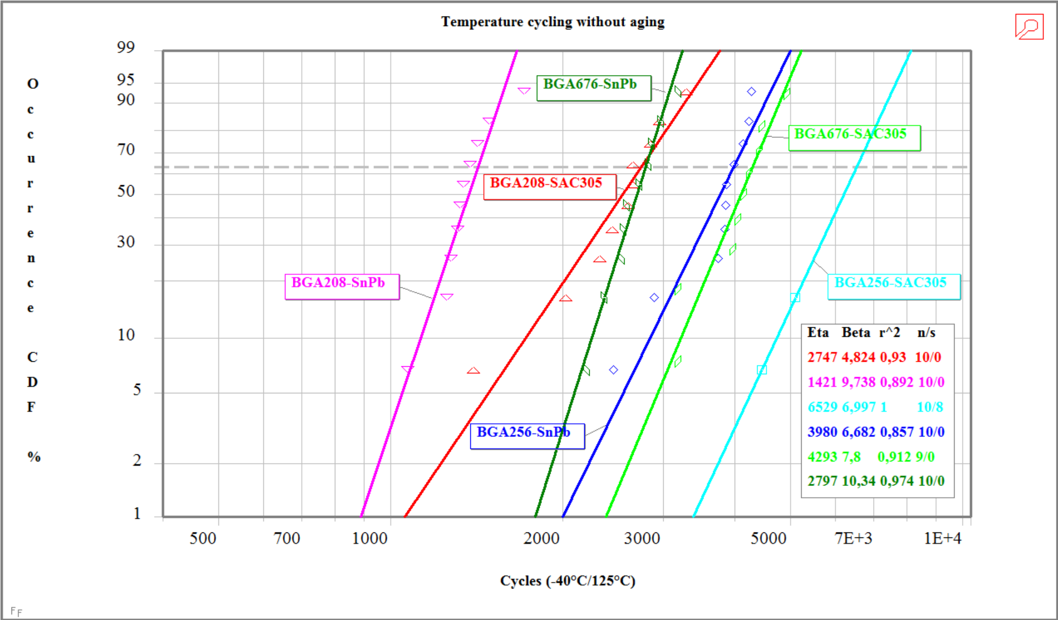

Fig. 4. Weibull plot for boards thermally cycled without prior aging for SAC305 and SnPb solder joints to HASL PCBs.

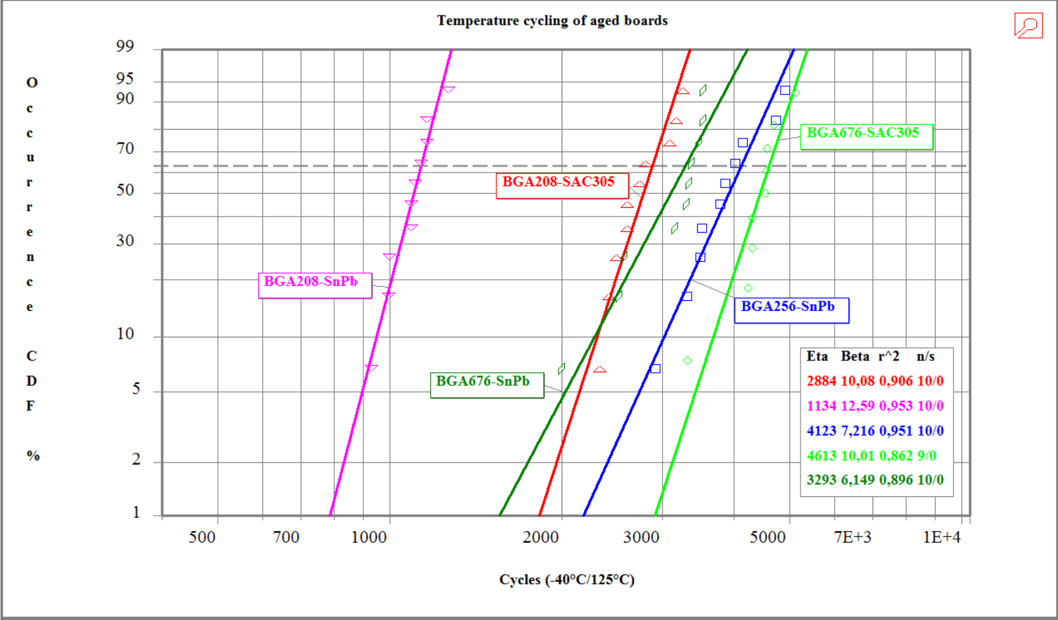

Fig. 5. Weibull plot for boards thermally cycled with prior aging for SAC305 and SnPb solder joints to HASL PCBs.

The calculated eta and beta values are summarised in Table 4. For all BGAs, the components with lead-free solder joints had considerably longer fatigue lives than those with SnPb solder joints, as reported by many others [2-4]. For the BGA208 component, the eta was about 100% larger for the components with lead-free solder joints and for the BGA676 component about 50% larger. The improvement in eta for the lead-free BGA256 was probably also at least 50% but, since only two failures occurred for the lead-free BGA256 component, this value is

uncertain. These results are somewhat surprising since the large chip in the BGA208 and the low stand-off for this component will cause a higher strain on the solder joints compared to the other two BGAs. Normally, that results in less difference in the fatigue lives for SnPb and lead-free components [1], and not the opposite as was observed in this study.

In most cases, aging prior to the thermal cycling test improved the fatigue lives with 3-18%. An exception was the BGA208 with SnPb solder joints for which aging prior to the thermal cycling test decreased the fatigue life with about 20%.

Table 4 Eta and beta values for the BGA components with lead-free and SnPb solder joints to HASL PCBs.

Board ID	BGA208		BGA256		BGA676	
	Eta (cycles)	beta	Eta (cycles)	beta	Eta (cycles)	beta
SAC, non-aged (2a)	2747	4.82	6529[a]	7.00	4293	7.80
SnPb, non-aged (2b)	1421	9.74	3980	6.68	2797	10.3
SAC, aged (3a)	2884	10.1	>5000[b]	-	4715	9.40
SnPb, aged (3b)	1134	12.6	4123	7.22	3293	6.15

[a] Value uncertain due to only two failures.

[b] No failures after 5167 cycles.

3.1.1 Comparison of the results for the BGA676

In Fig. 6, typical results from resistance measurements of the pairs of solder joints in the daisy chains for two BGA676 components are presented, one with SnPb solder joints and one with SAC305 solder joints. For the BGA676 component with SnPb solder joints, most of the solder joints in the rows closest to the edge of the chip failed, both in the rows beneath the chip and in the rows just outside the chip. A bit surprising, very few failures occurred in the outermost row with solder joints. For the BGA676 component with SAC305 solder joints, most of the failures occurred in the rows outside the chip with only one failed pair of solder joints in the row just beneath the chip edge. Except for some failures in the outermost row, the failures seem to be randomly distributed as reported by several others and discussed in the Introduction section. Both components in Fig. 6 were mounted on test boards that had not been aged prior to the thermal cycling test but the results were similar for components on the boards that were aged prior to the test.

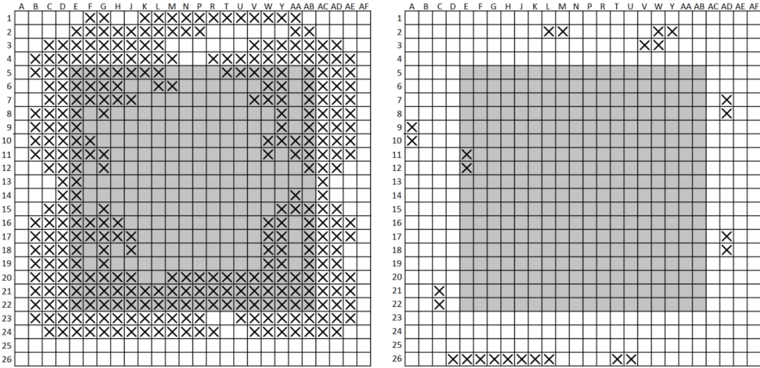

Fig. 6. Location of failed solder joints to BGA676 with SnPb solder joints (left image) and SAC305 solder joints (right image). The components were mounted on test boards that were thermally cycled without prior aging. Solder joint pairs with increased resistance or open circuit are marked with x. *The grey squares show the size of the chip in the component.*

Images of dye penetrant analysed BGA676 components are shown in Fig. 7 (not the same components as in Fig. 6). The results for the BGA676 with SnPb solder joints confirmed the results from the resistance measurements. Very few of the solder joints in the outermost row were completely cracked. Somewhat more solder joints were completely cracked in the second row whereas most of the solder joints were completely cracked in rows 3 to 7. All except a few of the completely cracked solder joints had cracked on the component side of the solder joints. However, removal of solder balls remaining on the PCB in rows 3 to 7 showed that there were also large cracks on the PCB side of the solder joints.

The cracks formed in the solder joints to the BGA676 with SAC305 solder joints were considerably smaller. Another difference was that about half of the solder joints broke at the PCB side of the solder joints. The extent of dye staining indicated that the formed cracks were of about the same size on the two sides of the solder joints. Also for the lead-free component, the cracks in the outermost rows were considerably smaller than in the other rows.

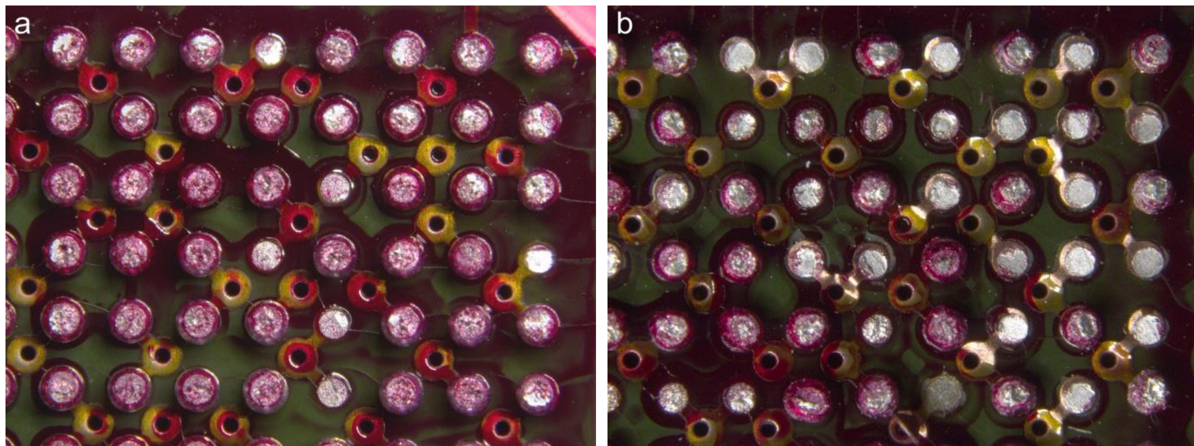

Fig. 7. Images of dye penetrant analysed BGA676 with a) SnPb solder joints and b) SAC305 solder joints. The components were mounted on test boards that were aged prior to the thermal cycling.

Cross-sections of solder joints in the outer row to BGA676 components with SnPb and SAC305 solder joints confirmed that the cracks in the lead-free solder joints were fewer and smaller than in the SnPb solder joints. In addition, for most of the solder joints to both components, cracks were also observed in the PCB laminate (Figs. 8 and 9). The laminate cracks had started at the edges of the solder pads and had in some cases grown in under the solder pads and in other cases away from them. The position of the glass weave in relation to the solder pads seemed to be important for determining the direction of the crack growth.

It can be noted that the stand-off of the solder joints in the outer row is larger for the SAC305 solder joints compared to the SnPb solder joints, 615 µm versus 575 µm. This is probably due to more extensive warpage of the lead-free BGA208 caused by the higher soldering temperature. Normally, a higher stand-off leads to a higher flexibility of the solder joints. Nevertheless, the cracks in the PCB laminate were slightly larger for the lead-free BGA676. The reason for the higher extent of cracking for the lead-free BGA208 is likely the higher elastic modulus of SAC305 solder compared to SnPb solder.

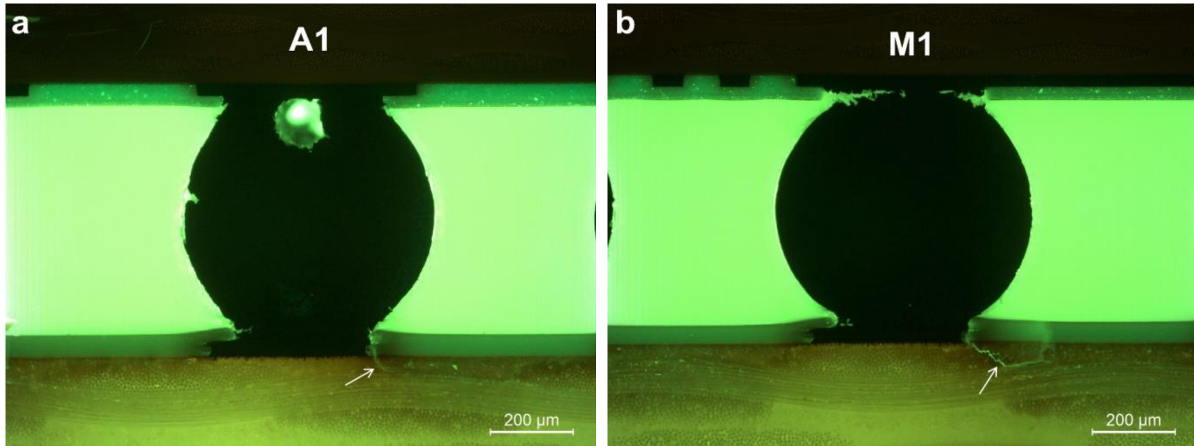

Fig. 8. *Cross-sections of solder joints a) A1 and b) M1 in the outer row of solder joints to a BGA676 with SnPb solder joints showing cracks in the PCB.*

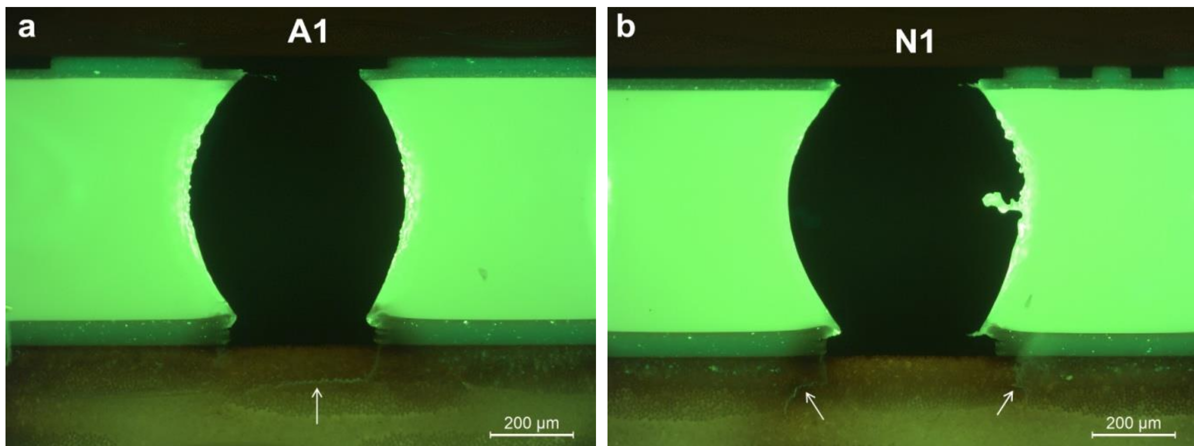

Fig. 9. *Cross-sections of solder joints a) A1 and b) N1 in the outer row of solder joints to a BGA676 with SAC305 solder joints showing cracks in the PCB laminate.*

3.1.2 Comparison of the results for the BGA256

The results for the BGA256 were similar to the results for the BGA676 except that much fewer solder joints with increased resistance were registered and the cracks in the solder joints were smaller. As for the BGA676 components, somewhat larger cracks were observed in the laminate for the lead-free component. One difference was observed, however. Between some of the solder joints to the lead-free BGA256, cracks were formed in the PCB laminate that more or less completely bridged between them (Fig. 10). The cracks were formed just under the PCB surface on top of glass fibre bundles aligned perpendicular to the cross-sectioned surface. It was only when a glass fibre bundle was located right in between the solder joints that the crack bridged between them.

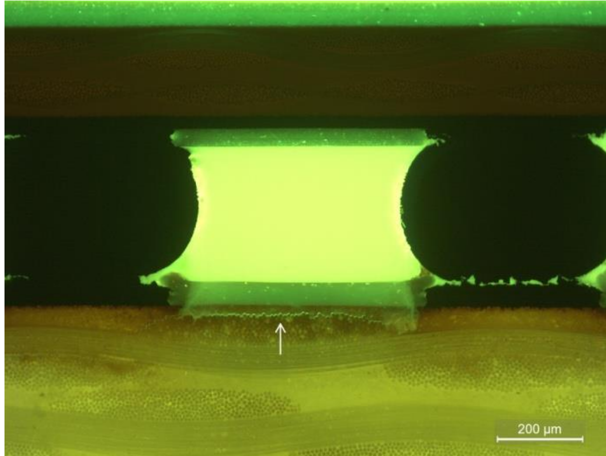

Fig. 10. Cross section of solder joints A16 and A15 in the outer row of solder joints to a BGA256 with SAC305 solder joints showing a crack in the PCB laminate between the solder joints.

3.1.3 Comparison of the results for the BGA208

Typical results from resistance measurements of the pairs of solder joints in the daisy chains for two BGA208 components are presented in Fig. 11, one with SnPb and one with SAC305 solder joints. For the BGA208 with SnPb solder joints, all pairs of solder joints beneath the chip had open circuits and only some pairs of the solder joints in the outer row of solder joints had unaffected resistance. The BGA208 with SAC305 solder joints had less affected solder joints but, also for this component, most of the affected solder joints were located beneath the chip.

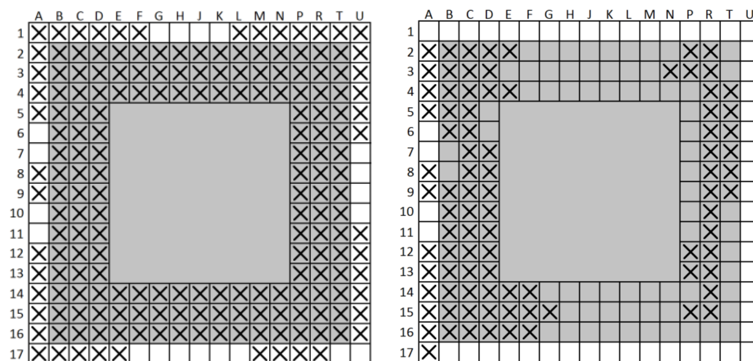

Fig. 11. Location of failed solder joints to BGA208 with SnPb solder joints (left image) and SAC305 solder joints (right image). The components were mounted on test boards that were thermally cycled without prior aging. Solder joint pairs with increased resistance or open circuit are marked with x. *The grey squares show the size of the chip in the component.*

An interesting result for the lead-free BGA208 components was that almost all solder joints that failed were located at two opposing sides of the components and were the same sides for all lead-free BGA208 components. This is probably due to the different CTE in the x- and y-directions for the PCB. In the cross-section shown in Fig. 10, the distance between the glass fibre bundles in the weave is about 0.57 mm whereas it is about 0.83 mm in Fig. 12 (taken perpendicular to the cross-section in Fig. 10). Likely, it is this difference in distance between the glass-fibre bundles in the x- and y-directions that cause the varying CTE in the two directions.

Cross-sections of solder joints in the outer row and in the second row (under the chip edge) to a BGA208 with SnPb solder joints are shown in Figs. 12 and 13, respectively. Most of the solder joints in the outer row and all solder joints under the chip in the second row were completely cracked and in most cases on the component side. Fig. 13a shows an example of an outer solder joint that was not completely cracked.

As for the BGA676 and BGA256 components, cracks were also observed in the PCB laminate. Very fine cracks could also be observed in the BGA laminate (Figs. 12b and 13b) but the number of cracks in the BGA laminate was less than in the PCB laminate. Most of the cracks in the PCB laminate formed at the edge of the opening in the solder mask but some cracks were also formed at the edge of the solder pads. This was not observed for the other BGAs since they had solder mask defined solder pads in contrast to the BGA208 that had non-solder mask defined pads. Cracks at the edge of the solder pads were mainly observed in the second row of solder joints. There were also somewhat more cracks in the PCB laminate in this row.

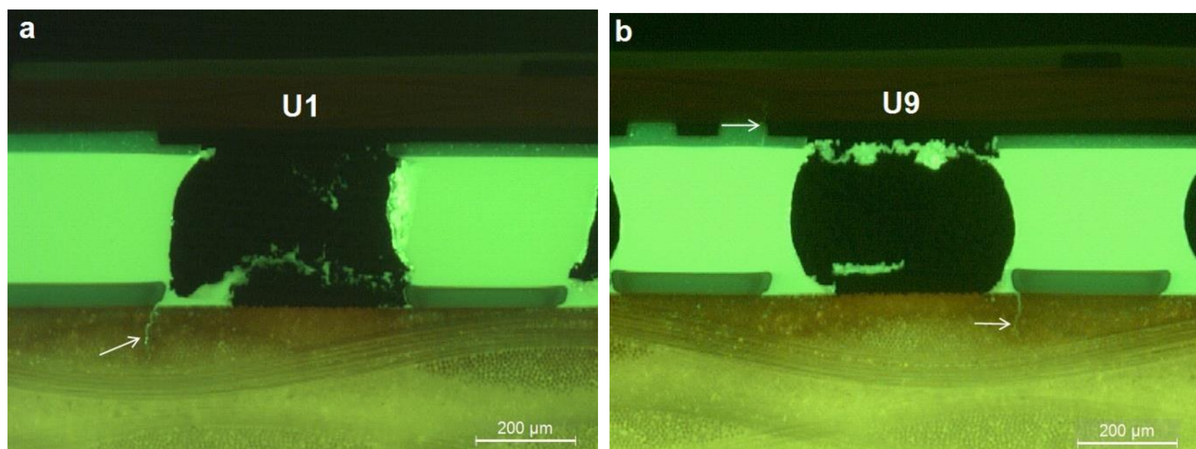

Fig. 12. Cross-sections of solder joints a) U1 and b) U9 in the outer row of solder joints to a BGA208 with SnPb solder joints showing cracks in the PCB. A crack in the BGA laminate can be observed for solder joint U9.

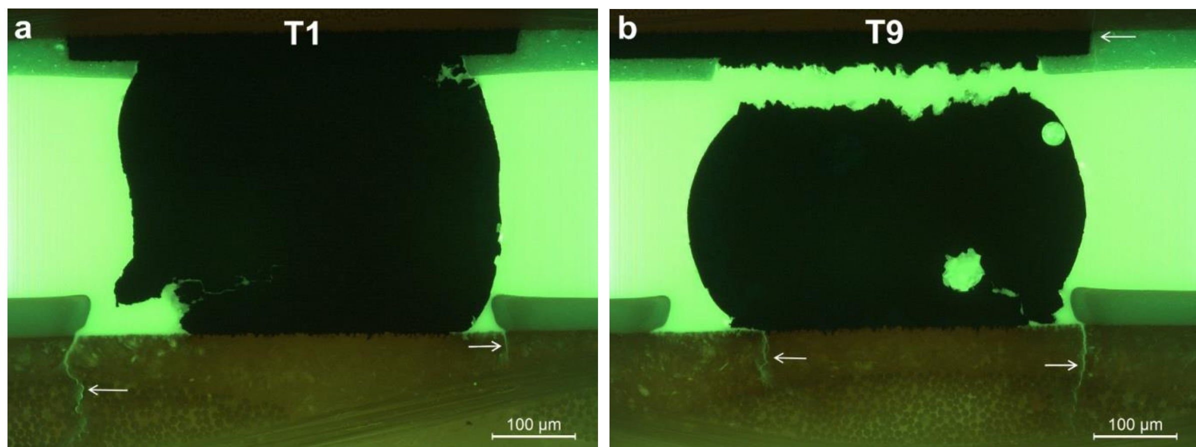

Fig. 13. Cross-sections of solder joints a) T1 and b) T9 in the second row of solder joints (under the chip edge) to a BGA208 with SnPb solder joints showing cracks in the PCB and BGA laminates.

Corresponding cross-sections for a BGA208 with lead-free solder joints are shown in Figs. 14 and 15. In the outer row, only one solder joint was completely cracked and that was a corner solder joint (Fig. 14a). Most solder joints in this row had only very small or no cracks at all. In the second row, most of the solder joints were completely cracked or had large cracks

whereas a few solder joints had only very small cracks (Fig. 15). The solder joints with very small cracks were located randomly and could be found next to a solder joint with a complete crack.

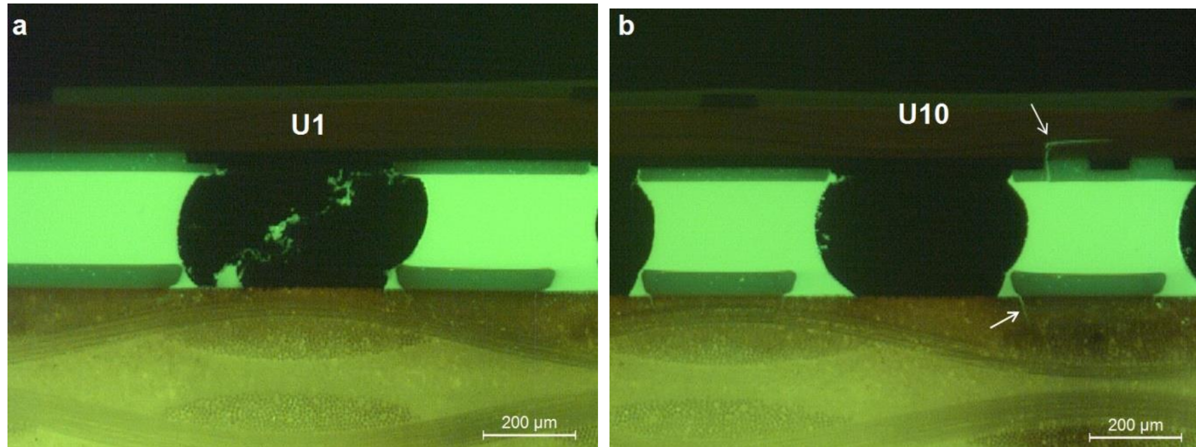

Fig. 14. Cross-sections of solder joints a) U1 and b) U10 in the outer row of solder joints to a BGA208 with SAC305 solder joints showing cracks in the PCB and BGA laminates.

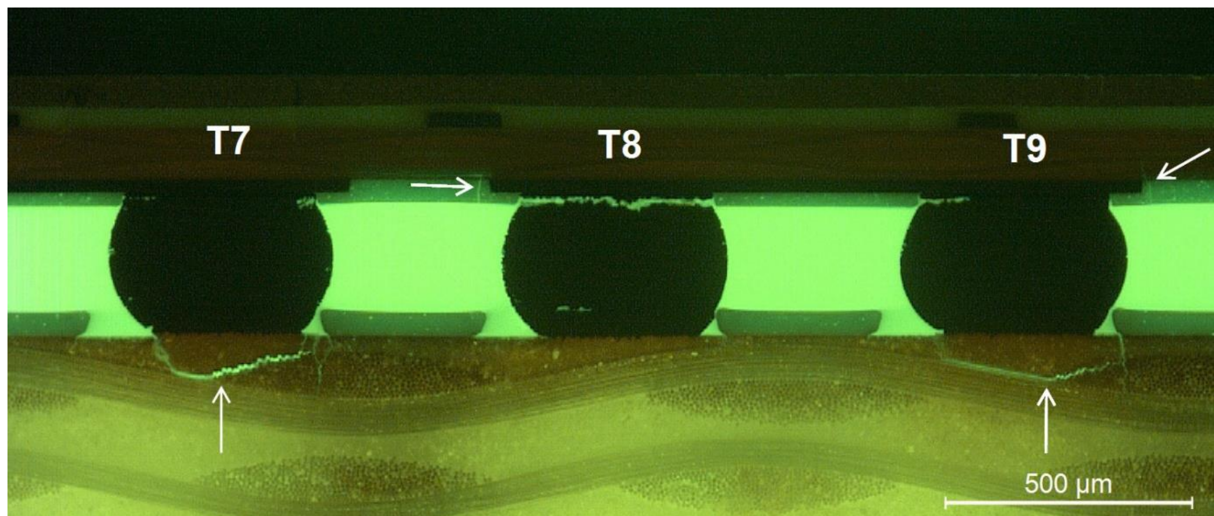

Fig. 15. Cross-sections of solder joints T7-T9 in the second row of solder joints to a BGA208 with SAC305 solder joints showing cracks in the PCB and BGA laminates.

The extent of cracking in the PCB laminate for the outer row of solder joints to the lead-free BGA208 was about the same as for the SnPb BGA208 (Figs. 12 and 14). In contrast, very large cracks were observed beneath two solder joints in the second row to the lead-free BGA208 (Fig. 15). These were found under solder joints that had only small cracks in the solder joints. No such large cracks were observed for the SnPb BGA208. There were also more and larger cracks in the BGA laminate for the lead-free BGA208 (Fig. 14) but some were still very fine (Fig. 16). In Fig. 16, an image of the cross-section taken with ordinary light is also shown to illustrate the difficulty to detect cracks in the laminates using optical microscopy if no fluorescent agent is added to the moulding compound and UV-light is used for the inspection. The upper part of the vertical crack in the PCB laminate to the right of the solder joint can be discerned (when you know it is there), but the rest of the crack in the PCB laminate and the crack in the BGA laminate are almost impossible to observe.

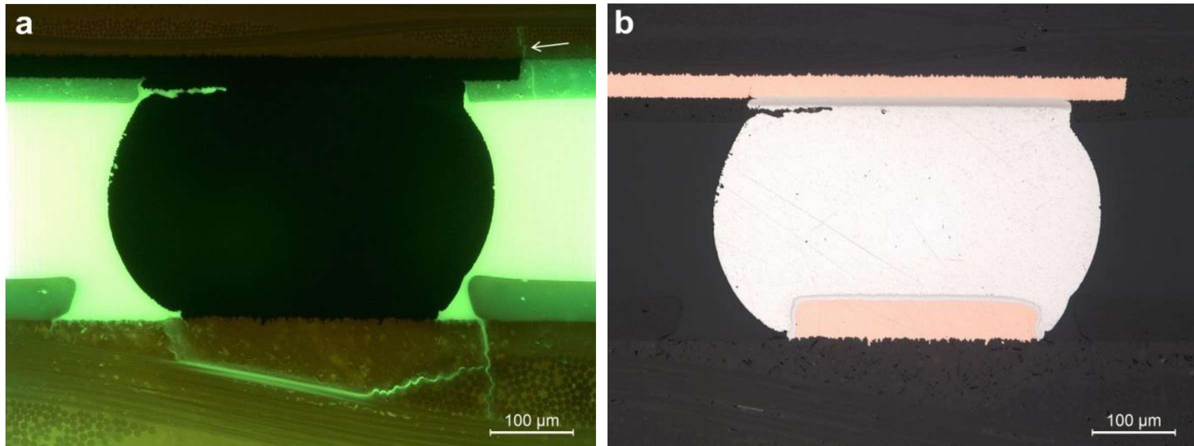

Fig. 16. *a) Image of solder joint T9 in Fig. 15 with larger magnification showing a very fine crack in the BGA laminate. b) Image of the same cross-section but taken with ordinary light.*

An alternative to use a fluorescent agent and UV light is to analyse the cross-sections using scanning electron microscopy (SEM). Using this technique, most cracks will be clearly discernible (Fig. 17).

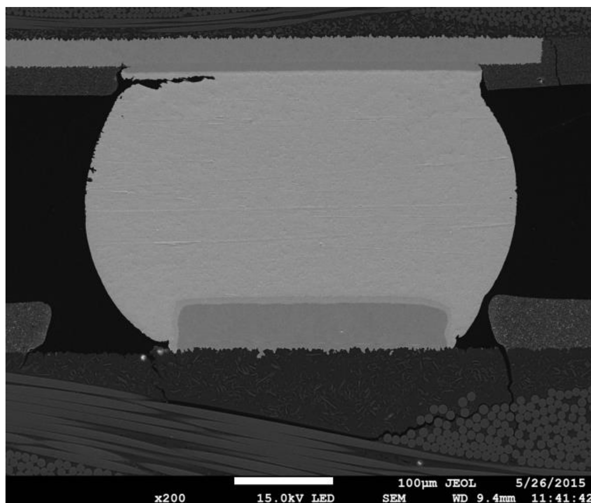

Fig. 17. *SEM image of solder joint T9 in Fig. 15.*

An interesting result is the very different behaviour of the three adjacent solder joints in Fig. 15. For the two solder joints with PCB laminate cracks, there are only small cracks in the solder joints. In contrast, for the middle solder joint, there is no crack in the PCB laminate but the solder joint is completely cracked. These three solder joints were analysed using electron backscatter diffraction (EBSD) in order to determine the number of grains in the solder joints and their orientation. Using this technique, grains with different orientations are shown with different colours. As shown in Fig. 18a-c, solder joints T7 and T9 consisted of single grains whereas solder joint T8 consisted of three large grains. Although there are streaks with orange colour in solder joint T7 indicating another unit cell orientation, the unit cell is the same as for surrounding areas except that it is rotated 180° around the a- or b-axes. Therefore, some disturbance in the uppermost layer has probably caused a misinterpretation of the unit cell in the orange area by the EBSD software.

There are also some small grains along the cracks but these have most likely been formed in a recrystallisation process during the thermal cycling and were not present at the beginning. The c-axis for the grain in solder joint T7 was close to perpendicular to the board surface. Also the

c-axis for the grain in solder joint T9 was mainly directed away from the board surface whereas the grains in solder joints T8 had very varying orientations.

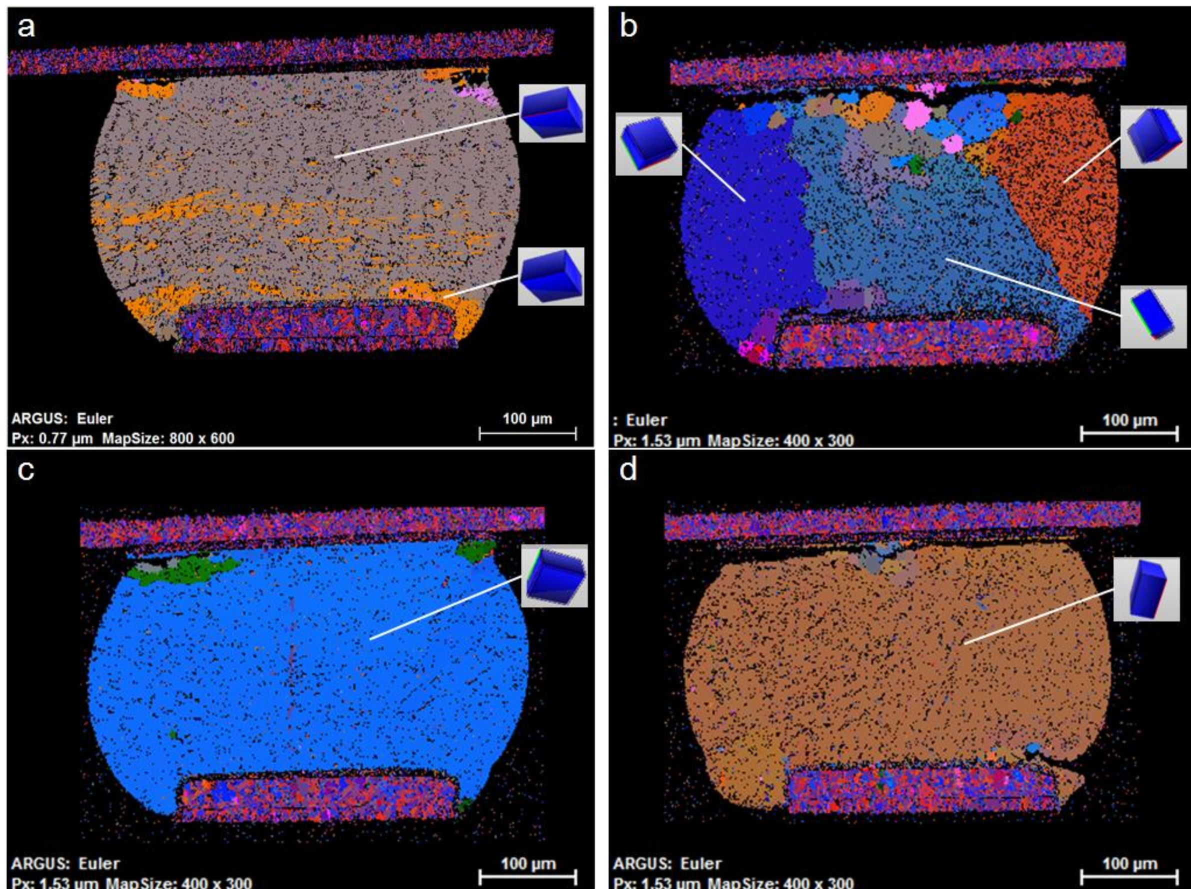

Fig. 18. EBSD images of solder joints a) T7, b) T8, c) T9 and d) T13 in the second row of solder joints to a BGA208 with SAC305 solder joints.

In addition to these three solder joints, also solder joint T13 is shown in Fig. 18d. It had an appearance similar to solder joint T8, i.e. a complete crack in the solder joint and no crack in the PCB laminate. Nevertheless, the solder joint consisted of only one single grain but, in this case, the c-axis was very close to parallel to the board surface but also to the cross-section plane.

3.2 Impact of various combinations of surface finish and solder paste

A Weibull plot with the results for all the BGA208 components soldered with the various combinations of surface finish and solder paste is given in Fig. 19. The calculated eta and beta values for these combinations are summarised in Table 5. It is striking that the beta values are much lower for the combinations of surface finish and solder paste that were soldered five months later than the combinations of SnPb/SnPb (finish/solder paste) and SN100C/SAC305. The lower beta values indicate a different failure mechanism or a mixture of two or more failure mechanisms. Whereas some of the components had fatigue lives that were well-matched with the SN100C/SAC305 combination, other components failed even earlier than the SnPb/SnPb combination. In fact, some components failed before 742 cycles. Due to a shortage of test channels, the boards that were soldered last were not connected to the event detector until after 742 cycles had been performed. Five components on these test boards had then already failed.

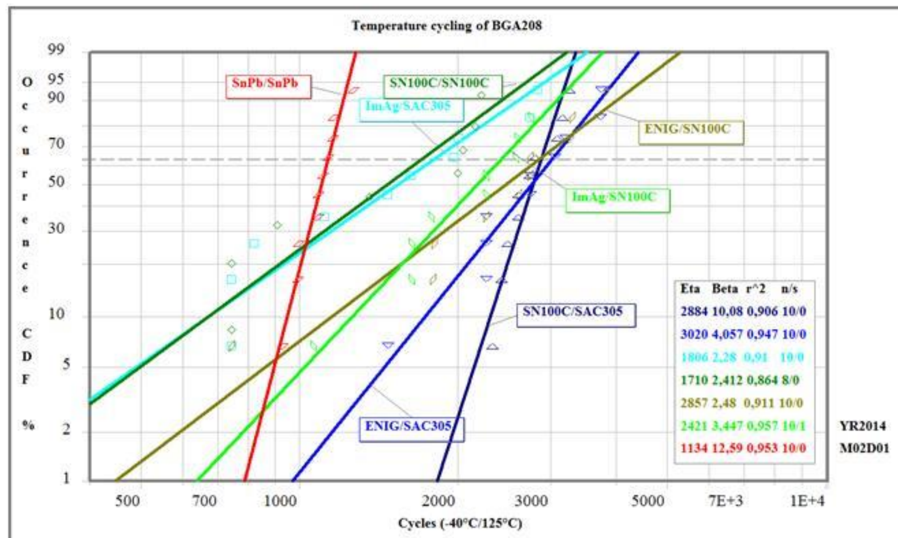

Fig. 19. Weibull plot for BGA208 components with various combinations of surface finish and solder paste on boards thermally cycled after aging.

Table 5 Eta and beta values for the BGA208 component for the various combinations of surface finish and solder paste.

Finish/solder paste	Eta (cycles)	Beta
SN100C/SAC305 (3a)	2884	10.1
ENIG/SAC305 (3c)	3020	4.06
ImAg/SAC305(3d)	1806	2.28
SN100C/SN100C (3e)	1710	2.41
ENIG/SN100C (3f)	2857	2.48
ImAg/SN100C (3g)	2421	3.45
SnPb/SnPb (3b)	1134	12.6

Localisation of failed pairs of solder joints by resistance measurements of the daisy chains showed that the numbers of failed solder joint pairs were less on these boards soldered five months after the first boards were soldered. That may mainly be due to the fact that they had passed through fewer thermal cycles (4030 cycles versus 5167 cycles). There was no clear difference in the number of failed solder joint pairs between components that failed early and components that failed late.

The combinations with SN100C/SN100C and ImAg/SAC305 had exceptionally low eta values and also several very early failures. Measurement of the stand-off for the BGA208 components and X-ray inspection indicated that the components that failed early for the SN100C/SN100C combination had higher stand-off compared to components that failed late. That was not the case for the components that failed early for the ImAg/SAC305 combination or for any of the other components on the boards with the other combinations of surface finish and solder paste.

One of the BGA208 components with the SN100C/SN100C combination that had failed after 742 cycles was analysed using the dye penetrant technique in order to determine if the early failure was due to the imperfect solder paste print for the BGA208 components. Only for nine of the solder joints, the solder joint broke at the interface between the solder and the solder pad on the PCB. In all these nine cases, the appearance of the fractures indicated that a proper solder joint had been formed. For many of the other solder joints, the solder pad was ripped

off from the PCB laminate. The appearance of many of these latter solder joints indicated poor wetting of the side of the NSMD solder pads.

In addition, a BGA208 with the SN100C/SN100C combination that failed after 908 cycles and had high stand-off was cross-sectioned (Fig. 20). The cross-section confirmed that the wetting on the side of many of the solder pads was indeed poor for this component. This resulted in a rather high stand-off of 290-320 µm (solder pad to solder pad distance). That can be compared with a stand-off of 220-225 µm for the BGA208 with the SN100C/SAC305 combination (see Fig. 16).

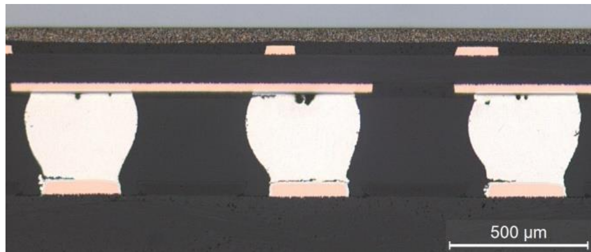

Fig. 20. Cross-sections of solder joints T8-T10 in the second row of solder joints to a BGA208 with the SN100C/SN100C combination that failed after 908 cycles taken with ordinary light.

Compared to the BGA208 with the SN100C/SAC305 combination, the solder joints under the chip edge to the component with high stand-off had more and larger cracks in the solder joints. Another difference was that for the SN100C/SN100C combination, the majority of the cracks were located close to the PCB side of the solder joints, whereas most cracks for the SN100C/SAC305 combination were located close to the component side. The non-symmetric shape of the solder joints for the SN100C/SN100C combination with a smaller diameter at the PCB side is likely the reason why the cracks were mainly formed there.

For most of the solder joints with the SN100C/SN100C combination, small vertical cracks were observed in the PCB laminate (Fig. 21a) and, for two of them, the cracks grow in under the solder pads (Fig. 21b). Although these horizontal cracks were rather large, they were considerably smaller than the largest cracks for the BGA208 with the SN100C/SAC305 combination. A few cracks were also observed in the BGA laminate for this component (Fig. 21b).

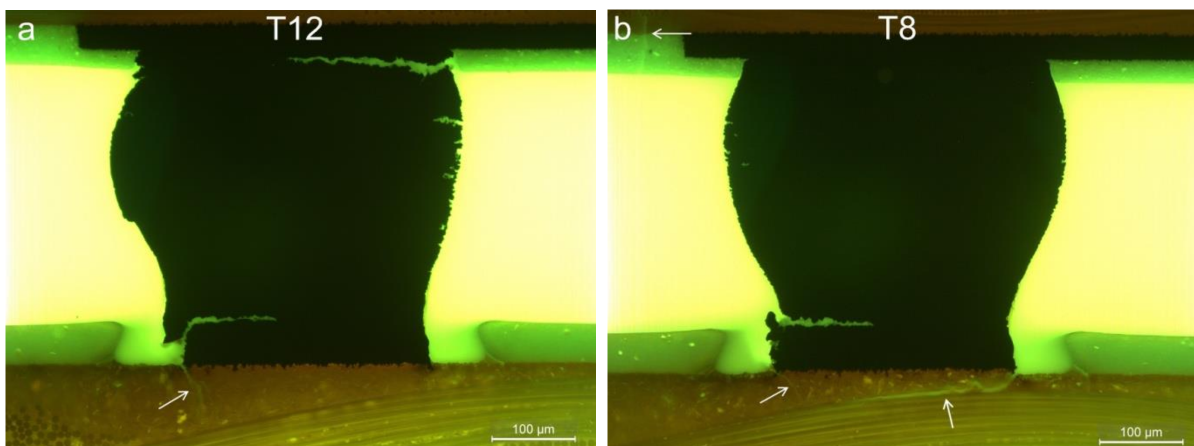

Fig. 21. Cross-sections of solder joints a) T12 and b) T8 in the second row of solder joints to a BGA208 with the SN100C/SN100C combination that failed after 908 cycles showing cracks in the PCB and BGA laminates.

A dye penetrant analysis was also carried out for a BGA208 with the ImAg/SAC305 combination that had failed after 1115 cycles. The appearance of the fractures indicated that proper solder joints had been formed also to this component. For solder joints where the solder pads were ripped off from the PCB laminate, the solder seemed to have completely wetted the sides of the solder pads. X-ray inspection of a component that failed before 752 cycles also indicated good wetting of the side of the solder pads and a small stand-off of the component.

A cross-sectioning of the second row on one side to a BGA208 with the ImAg/SAC305 combination that failed after 1631 cycles confirmed that the side of the PCB solder pads had been wetted (Fig. 22). The stand-off was 230-240 µm for non-cracked solder joints, which was only slightly higher than for the BGA208 soldered with the SN100C/SAC305 combination which had a stand-off of 220-225 µm. As for the BGA208 with the SN100C/SN100C combination, most solder joints had large cracks. A difference was that most of the cracks for the ImAg/SAC305 combination were located close to the component side of the solder joints, similar to the SN100C/SAC305 combination.

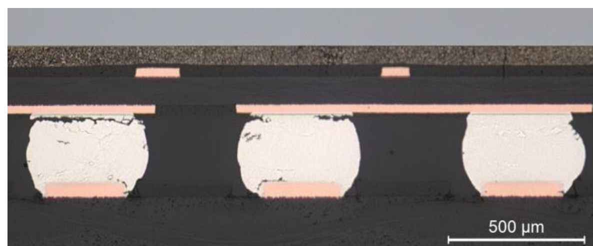

Fig. 22. Cross-sections of solder joints T4-T6 in the second row of solder joints to a BGA208 with the ImAg/SAC305 combination that failed after 1631 cycles.

Apart from these observations, the results for the ImAg/SAC305 combination were similar to the results for the SN100C/SN100C combination. Small vertical cracks were observed in the PCB laminate for most solder joints. In most cases, large cracks were observed in the solder joints but not for all (Fig. 23a). Only one of the 17 solder joints in the cross-section had a laminate crack that had grown under the solder pad but, on the other hand, that was a very large crack (Fig. 23b). For this solder pad, the distance between the pad and the glass weave was very short which may have facilitated the crack formation.

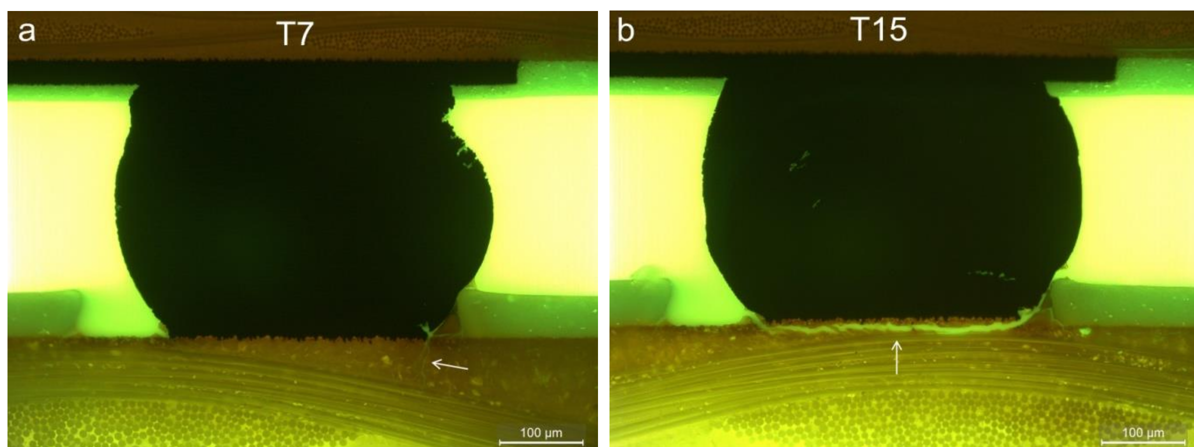

Fig. 23. Cross-sections of solder joints a) T7 and b) T15 in the second row of solder joints to a BGA208 with the ImAg/SAC305 combination that failed after 1631 cycles showing cracks in the PCB laminate.

4 Discussion

4.1 Origin of the laminate cracks

It is a possibility that the laminate cracks formed during the preparation of the samples for the cross-sectioning and then especially when the samples were cut out from the boards. To prevent that, the samples were cut out very carefully but it is still a possibility that the cracks were formed then. However, it is very unlikely that the cutting would cause much larger laminate cracks under the solder pads in the second row than in the first row as was observed for the BGA208 component with the SN100C/SAC305 combination (see Figs. 14 and 15). This was also observed for a dye penetrant analysed component (Fig. 24). Several of the solder pads were ripped off from the PCB when the component was removed revealing extensive red staining of the PCB laminate under the pads in the second and third rows but not in the first row. Therefore, it is not likely that the cracks were formed during the cutting out of the samples for the analysis.

Fig. 24 Image of dye penetrant analysed BGA208 component with the SN100C/SAC305 combination showing the upper left corner of the footprint on the PCB after the component had removed.

4.2 Impact of laminate cracks on solder joint fatigue

Cracks in the PCB laminate were observed for all BGAs. For some BGAs, cracks were also observed in the BGA laminate. The cracking in the PCB laminate was more severe for components with lead-free solder joints compared to SnPb solder joints. Especially severe laminate cracking was observed under some of the solder joints located beneath the chip for the lead-free BGA208 components. Since such cracks in the PCB and BGA laminates will reduce the stress on the solder joints by increasing their flexibility, they will improve the fatigue life of the solder joints. The larger the cracks, the more will the fatigue life be improved.

A survey of the fatigue lives reported in the literature for BGA208 and BGA288 components having 0.8 mm pitch (Table 6) revealed that the reported fatigue lives varied considerably. Notably and surprisingly, the component having the largest chip was reported to having the longest fatigue life, both for SAC305 and SnPb solders. Furthermore, this component was

mounted on a rather thick PCB which normally is detrimental for the fatigue life of solder joints [25]. It is also the most recently performed investigation of the investigations referred to in Table 6. PCB laminate cracking may explain the unexpected long fatigue lives reported in that investigation. Thus, the results reported in the literature indicate that cracking of the PCB laminate may have influenced the fatigue lives of the solder joints in some of the investigations (although cracks were not reported) and that the risk for laminate cracking has increased in recent years.

Table 6 Reported fatigue lives for BGA208 and BGA288 components having 0.8 mm pitch. All were thermally cycled between -40°C and 125°C except the FPBGA208 which was thermally cycled between -55°C and 125°C

Component	Chip size	PCB thickness	Solder	Eta (cycles)	Ref.
CABGA208	?	2.4 mm	SAC305	1774	22
fleXBGA208	9.5 mm	1.6 mm	SnPb	2352	25
fleXBGA208	12.0 mm	1.6 mm	SnPb	708	25
PBGA208	12.7 mm	2.4 mm	SAC305	3422-3743[a]	26
PBGA208	12.7 mm	2.4 mm	SnPb	3413	26
FPBGA208	11.4 mm	1.6 mm	SnPb	~400	27
PBGA288[b]	?	2.4 mm	SAC405	~1300	28
PBGA288[b]	?	2.4 mm	SnPb	~1000	28

[a] Two different finishes on the PCB solder pads.

[b] Package body size 19 mm x19 mm.

4.3 Impact of tin anisotropy on laminate cracking

One interesting result for the lead-free BGA208 components was that the behaviour could be very different for adjacent solder joints. This was most pronounced for solder joints located under the chip. This difference in behaviour can be explained by the anisotropy of tin grains. Thermo-mechanical fatigue of solder joints is caused by stress-induced creep as a result of cyclic changes in temperature. The stresses solder joints are exposed to can be split into stresses caused by global, local and internal CTE mismatches. Stress caused by global CTE mismatch is caused by the CTE mismatch between a component and the PCB. It increases with increasing CTE mismatch, delta T and distance from the centre of the component but, likely, it is not affected much by the number of tin grains and their orientation in lead-free solder joints.

The local CTE mismatch is caused by the CTE mismatch between the solder and the solder pads/laminates which will cause stresses at the corresponding interfaces. In this case, the orientation of a tin grain in a single-grained SAC solder joint will have a large impact on the resulting stresses. At ambient conditions, the CTE along the a- and b-axes in a tin grain (about 15 ppm/°C) is at the same level as the CTE of copper (16-17 ppm/°C [11, 15, 29]) and of the PCB and BGA laminates in the x- and y-directions (about 12-18 ppm/°C [14, 15, 30]). Therefore, if the tin grain is oriented with the a- and b-axes parallel to the board surface, the stresses at the interfaces will be low. On the other hand, since the CTE along the c-axis in a tin grain is about 30 ppm/°C, the CTE mismatch will be about 15 ppm/°C if the tin grain is oriented with the c-axis parallel to the board surface. Whereas the CTE of copper is fairly independent of the temperature [29] and probably also for the PCB, the CTE of tin is strongly affected by temperature. At 125°C, the CTE of tin is about 20 ppm/°C along the a- and b-axes and about 40 ppm/°C along the c-axis [11]. That will result in a CTE mismatch to the pads of 20-25 ppm/°C in the worst case. Furthermore, if the solder pad on the BGA laminate is

located beneath the chip, the very low CTE of the chip will reduce the expansion of the solder pad which will lead to an even higher CTE mismatch on the component side of the solder joint [7]. That may contribute to the observations that most cracks in the solder joints usually are formed on the component side.

For solder joints consisting of more than one grain, there will be an internal CTE mismatch between the grains which will depend on their orientation. The mismatch may be up to 15-20 ppm/°C, which will cause a high internal stress at the grain boundaries which will facilitate formation of fatigue cracks [7, 13]. This is to some extent also the case for SnPb solder joints, but the tin grains are then mixed with much softer lead grains [7, 11] and the general grain size is much smaller. Therefore, the impact of internal stresses is much smaller in SnPb solders [7].

In addition, due to the anisotropy of tin grains, a special case of CTE mismatch occurs for SAC solder joints to BGAs. For a single-grained solder joint oriented with the c-axis parallel to the board surface, the CTE of the solder joint in the direction perpendicular to the board surface will be lower than for the surrounding solder joints unless they all are single-grained solder joints with the c-axis parallel to the board surface [8]. This will cause a tensile stress on the single-grained solder joint with the c-axis parallel to the board when temperature is increased, and a compressive stress when temperature is decreased. The opposite will be the case for the surrounding solder joints.

The global CTE mismatch is usually much more important for the fatigue life of SnPb solder joints than the local and internal CTE mismatches, but the situation is different for SAC solder joints due to the anisotropy of tin. As discussed, single-grained solder joints having the c-axis parallel with the board surface will have a substantial local stress close to the solder pads and these solder joints have been found to be much more likely to crack even if they are not the solder joints with the largest global mismatch [8, 11]. Nevertheless, the global CTE mismatch will also be important for the total stress level on a solder joint. That is, a single-grained solder joint having the c-axis parallel with the board surface will be more likely to fail if it is far away from the centre of the component compared to if it located close to the centre.

Probably, the number of grains and their orientation in neighbouring solder joints will also to some extent affect the fatigue life of the solder joints due to the alternating tensile and compressive stresses that they will cause. However, not only the solder joints will be exposed to these tensile and compressive stresses but also the laminates in the PCB and the BGA. If a single-grained solder joint having the c-axis perpendicular to the board surface is surrounded mainly by multi-grained and/or single grained solder joints having the c-axis parallel to the board surface, then it will be exposed to high tensile and compressive stresses when cooled and heated, respectively. If the stress is high enough, it may cause a crack to form in the PCB laminate beneath the solder pad. The high elastic modulus along the c-axis (three to four times higher than along the a- and b-axes [8]) will also contribute to that high stress is transferred to the PCB laminate. Since the c-axes for the single-grained solder joints T7 and T9 in Fig. 18 were close to perpendicular to the board surface, this is probably what caused the formation of the large cracks in the PCB laminate beneath these solder joints.

The PCB laminate will also be exposed to shear stress due to the global CTE mismatch. The further away a solder joint is from the centre of the component, the larger will the shear stress be. Due to the higher elastic modulus along the c-axis, the shear stress which the PCB laminate will be exposed to will also be affected by the orientation of the tin grains. For a single-grained solder joint having the c-axis parallel to the board surface, the shear stress on the PCB laminate will be higher if the c-axis is pointing to the centre of the component compared to if it is turned 90° (as in Fig. 18d).

Therefore, for SAC solder joints located under the chip of the BGA208 component, the stresses on the solder joints and the laminates can be expected to vary considerably for adjacent solder joints due to the anisotropy of the tin grains. That not only explains why a solder joint with no cracks in the PCB laminate could be found between two solder joints with extensive cracking in the PCB laminate but also why the solder joints that fail first are to a large extent randomly located.

In previously performed studies of ceramic BGAs with Sn10Pb balls soldered to Thermount 85NT and polyimide/glass PCBs, cracking beneath the solder pads was always initiated on the side of the solder pads that faced the centre of the component [18, 19]. All cracks then grew in under the solder pads. The cross-sections carried out in those studies were done along the diagonal of the components. Since the cross-sections carried out in this study was done parallel to an edge of the components, it is more difficult to tell were the cracks were initiated although cross-sections of solder joints near corners of the components indicate that many of the cracks were initiated on the side facing the centre of the components. Nevertheless, the cracks in the PCB laminate seem to be more randomly formed in this investigation with some cracks growing in under the solder pads and other cracks growing away from the solder pads. The complex stress distribution with some solder joints being under combined shear and tensile stresses at the same time as adjacent solder joints being under combined shear and compressive stresses may be the reason for this deviant distribution of the cracks. The location of the cracks and the extent of crack growth under the solder pads, however, are also dependent on the location and orientation of glass fibre bundles with respect to the solder pads [20]. For example, the formation of the crack shown in Fig. 23b has probably been facilitated by the very short distance between the solder pad and the underlying glass fibre bundle.

4.4 Impact of laminate properties and soldering on laminate cracking

Since the tested PCBs were produced using only one laminate material, it is not possible to determine to what extent the laminate properties have affected the formation of the laminate cracks. However, it is possible or even likely that the test boards used have been especially prone to form laminate cracks. The PCB laminate used was a phenolic-based high T_g and high T_d material with low CTE developed to withstand lead-free soldering and to generate low stress on through-hole platings. The properties are achieved by using a resin with a high degree of cross-linking and a high content of inorganic fillers. This result in a laminate with a high elastic modulus but also a laminate that is more brittle than traditional low T_g laminates [21, 31]. The higher elastic modulus will result in higher stress levels both in the solder joints and in the PCB laminate during thermal cycling. This in combination with the higher brittleness contributes to making the material more susceptible to laminate cracking when exposed to stress. Nevertheless, the extent of laminate cracking, and the fact that cracks also formed in the BGA laminate, indicate that cracking in the PCB laminate is likely to occur to some extent also for other laminates during thermal cycling of assemblies with BGAs.

The highest thermo-mechanical stress that solder joints will be exposed to will occur during the cooling phase after soldering. Hence, it is possible that the laminate cracks that formed beneath the solder joints most susceptible to laminate cracks were initiated in the soldering process. Even very small cracks initiated in the laminate during soldering can possibly change the failure mode from fatigue cracking of the solder joints to laminate cracking [32]. In fact, it has been shown that pre-stress on the laminate prior to a thermal cycling test may cause latent damages in the laminate which cannot be observed as cracks in cross-sections, but nevertheless increase the risk for laminate cracking in a subsequent thermal cycling test [23].

Soldering processes increase the hardness of PCB laminates due to the exposure to high temperature [20, 33]. A higher hardness probably makes the laminate more brittle and thus more vulnerable to laminate cracking. The increase in hardness is higher in lead-free soldering due to the higher soldering temperature [33]. Since HASL is basically a soldering process, where the PCBs actually are exposed to even higher temperatures than during assembly, HASL can be expected to increase the susceptibility to laminate cracking, especially for lead-free HASL. That may explain the shorter fatigue lives for the solder joints to the BGA208 components mounted on the non-HASL boards. If the laminate is less prone to laminate cracking, fewer and smaller laminate cracks will form. The stress will then be higher on the solder joints resulting in a shorter fatigue life. It may also explain the longer fatigue lives for the samples that were aged prior to the thermal test. The aging would also make the laminate more brittle resulting in more and larger laminate cracks and, thereby, longer fatigue lives of the solder joints.

The lead-free HASL PCBs soldered with SN100C solder paste that were soldered five months after the lead-free HASL PCBs soldered with SAC305 solder paste had also a rather short fatigue life for the BGA208, at least for some of the components. These components had poor wetting on the sides of the solder pads. Non-solder mask defined pads with lead-free HASL have a very thin coating with SN100C at the edges of the pads. When stored, the thin tin layer at the pad edges may be completely consumed forming tin-copper intermetallics. That will make it more difficult to wet the sides of the solder pads resulting in a higher stand-off if the sides of the pads are not wetted. The low solder paste volume printed on the solder pads may also have contributed to the difficulty to wet the sides of the solder pads. Normally, a higher stand-off would lead to improved fatigue life due to higher flexibility of the solder joint but the opposite was observed for these components. There may be two explanations for this behaviour. Due to the poor wetting on the sides of the PCB solder pads, the diameter of the solder joints decreased at the PCB side of the solder joints. This will make the solder joints more susceptible to fatigue on this side. Since the failure location was shifted to the PCB side of the solder joints, the reduced diameter of the solder joints at the PCB side may the reason for the shorter fatigue life. Alternatively, the higher flexibility of the solder joints may have led to that fewer and smaller cracks were formed in the PCB laminate, which was actually observed. As a consequence, the fatigue life would become shorter. In this case, the shorter fatigue life for some of the components would be due to the higher stand-off of them.

However, the results for the non-HASL boards showed large variation in eta and beta values indicating that also other factors may affect the results. In fact, the ENIG/SAC305 combination had even a higher eta value than the SN100C/SAC305 combination although the beta value was much lower. In this case, the much higher elastic modulus of the nickel plating on the solder pads may have caused more stress to be transferred to the PCB laminate resulting in more cracking of the laminate.

4.5 Impact of laminate cracks on the interpretation of results from thermal cycling

The results from this investigation have a large impact on how to interpret results from thermal cycling of area array components. In order to correctly interpret the results, it is important to clarify to what extent cracking may have occurred in the PCB and BGA laminates. Since fine cracks in the laminates may be difficult to observe in cross-sections, moulding should be done using moulding compounds with an added fluorescence agent to facilitate the detection of cracks in the laminates. Alternatively, inspection should be done using SEM.

If cracks are formed in the laminates, it indicates that cracks may form in assemblies if they will be used in field conditions with a temperature exposure similar to the thermal cycle used in the test. It will improve the fatigue lives of the solder joints but it may cause other types of failures and then mainly formation of Conductive Anodic Filaments (CAF) and fracturing of copper tracers connecting the solder pads or fracturing of via-in-pad [19, 33, 34]. Although the risk that laminate cracks will cause these types of failures may be small [33], they need to be considered. Since there is no standard that has acceptance criteria for this type of cracks in the laminates, it is up to each producer/buyer to determine what is acceptable.

The likelihood for cracks to develop in the laminates when exposed to temperature changes decreases with decreasing delta T. Therefore, if cracks are formed in a thermal cycling test and a product will be used in more benign conditions, it will be difficult to estimate the fatigue lives in these conditions. The test results may lead to grossly overestimated fatigue lives as the results from this study show. Cracks in the PCB laminate were observed for all BGAs, both for SnPb and lead-free solder joints but the cracks were larger for the lead-free solder joints. The solder joints that are most likely to cause cracks in the PCB and BGA laminates are probably those that would be the first to develop fatigue cracks if no cracking would occur in the laminates. Consequently, the fatigue lives of the lead-free BGA208 components can be expected to have been much shorter if the cracking of the PCB and BGA laminates had not occurred.

Thus, if one would try to estimate the fatigue lifetimes in more benign conditions from the results in this investigation, they will be overestimated and most for lead-free BGAs. The overestimation would perhaps not be so much for the BGA256 and BGA676 components but it is not possible to tell from the results in this investigation how large the overestimation would be. However, the results for some of the BGA208 components soldered to non-HASL PCBs with relatively small laminate cracks that failed before 742 cycles indicate the overestimation may be at least a factor of three for the lead-free BGA208. Note that a few relatively large cracks were also formed in the PCB laminate for a BGA208 that failed very early (Fig. 21). That is, the fatigue life for this lead-free BGA208 may indeed have been considerably shorter if no cracks in the laminate had formed.

To avoid that cracks are formed during thermal cycling, it may be necessary to decrease the delta T in the test. The drawback is that it will necessitate longer test times. For products used in relatively harsh conditions with long expected lifetime, for example electronics in automotive compartments or truck cabs, it may require test times of more than one year. Still, even if the delta T in the test is decreased, there is a risk that some cracking will occur for the solder joints that are most susceptible to form PCB laminate cracks, i.e. solder joints located under the chip for BGAs with low stand-off. For these components, there will inevitably be a risk for an overestimation of the fatigue life of the solder joints if the delta T in the test is larger than the delta T in the field conditions. To rule out that cracking in the PCB laminate has affected the results for these components, it would be necessary to cross-section all solder joints to the BGAs, at least the solder joints located under the chip.

Thus, many of the results reported in the literature from thermal cycling of area array components may to some extent have been affected by the formation of cracks in the laminates, especially if solder joints are located under the chip. This is in particular true for results reported during the last five to ten years. There are many contributing factors to this. The most important is the transition to lead-free soldering. Since lead-free solder joints are considerable stiffer than SnPb solder joints, the lead-free solder joints will transfer considerably more stress to the PCB laminate. The existence of single-grained SAC solder joints makes the situation even worse. Also, the transition to low-CTE moulding compounds has increased the global CTE mismatch leading to more stress on the laminate. Furthermore,

in order to make PCB laminates more resistant to lead-free soldering, new laminates with higher T_g, T_d and filler content have been developed. The higher soldering temperature used in lead-free soldering will contribute to an increased hardness of the PCB laminate. The price to be paid for these changes is a higher elastic modulus and lower fracture strength, both contributing to making the laminate more susceptible to laminate cracking. Decreasing pitch for BGA components leading to shorter stand-off will also increase the stress on the PCB laminate.

4.6 Implications on the assessment of solder joint reliability

All these factors increasing the risk for laminate cracks may have a very large negative impact on the fatigue lives of the solder joints if cracks are not formed in the PCB laminate. The percentage of solder joints to a BGA that are single-grained may vary between 20 and 85% depending on the surface finish on the PCB [12, 15]. The lowest percentage of single-grained solder joints to BGAs is observed for PCBs with HASL finish [12]. According to Bieler et al. [8], about 25% of single-grained SAC solder joints may have an orientation of the c-axis that is close to parallel with the board surface, i.e. the orientation that will cause most local stress on the solder joints. For these, only some will have the c-axis pointing to the centre of the component, i.e. the orientation that will transfer most shear stress to the laminate. Even fewer than 25% of the single-grained solder joints may have an orientation of the c-axis that is close to perpendicular to the board surface, i.e. the orientation that will cause most tensile/compressive stress on the PCB laminate.

Accordingly, each solder joint to a BGA will have a set of neighbouring solder joints with quite varying number of grains and orientation of these. Therefore, each solder joint to a BGA will have a unique stress situation. Consequently, the spread in failure distribution can be expected to be high for BGAs soldered with SAC solder, i.e. a low beta value in a Weibull plot. As pointed out by Bieler et al. [7] and Lehman et al. [17], some components can be expected to have a very unfavourable combination of stresses on the solder joints located under the chip corners. These may cause quite early failures, earlier than predicted by a Weibull plot. This is of large concern for products with long expected service life and very low acceptable failure levels.

A low beta value and an early failure were indeed observed in this investigation for the lead-free BGA208 component on the boards that had not been aged prior to the thermal cycling test (Fig. 4). Low beta values and early failures have also been reported in other investigations of the fatigue lives of lead-free BGAs [3, 4, 28, 35-37]. However, it is not observed in most investigations. For some of these investigations, it may be due to that cracking of the PCB laminate has occurred.

The results from this investigation do not only affect how to interpret the results from thermal cycling, it affects also the basis for reliability simulations. As stated by Bieler et al. "*Certainly failure rates determined on the basis of prevalent microstructures cannot be construed to be representative of the behaviour of all Pb-free, near eutectic SAC solder joints in a package. Rather, minority orientations that are susceptible to damage nucleation need to become the basis for reliability prediction*" [7]. Variations in tin grain size and grain orientation in solder joints must be examined, quantified and understood in order to anticipate and predict the reliability of BGAs with lead-free solder joints, but that is not enough. The impact of grain size and grain orientation in solder joints on laminate cracking must also be examined, quantified and understood to enable adequate reliability simulations. In addition, the fracture strength of the laminates and the impact of the position of the glass weave in relation to the solder pads must also be considered. That will make reliability simulations a true challenge.

5 Conclusions

Thermal cycling of assemblies with BGAs may cause formation of cracks in the PCB laminate and, to a lesser extent, in the BGA laminate for plastic BGAs. The cracks are formed at or under the solder pads. They may be hard to detect in optical inspection of cross-sections if not moulding compounds with added fluorescent agents are used and the inspection is done using UV-light.

Since the cracks increase the flexibility of the joints, they will improve the fatigue lives of the solder joints. The results from this investigation indicate the improvement in fatigue life may in some cases be a factor of three or more. As a consequence, the fatigue life of a BGA that will be exposed to smaller temperature variations in field conditions than in a thermal cycling test may be grossly overestimated.

A large number of changes in the manufacture of assemblies during the last 5-10 years has increased the risk for that this type of laminate cracks are formed. The most important is the transition to lead-free soldering. Lead-free solders have higher elastic modulus than SnPb solders and, therefore, will transfer more stress to the laminate. Another ongoing change that increases the risk for laminate cracking is the decreasing pitch for BGAs leading to shorter stand-off. The risk for laminate cracking is especially large if the solder joints are located under the chip. Transition to low-CTE moulding compounds for encapsulation of plastic components and new PCB laminates with higher T_g, T_d and filler content have also contributed to an increased risk for laminate cracks. The new moulding compounds because they increase the CTE mismatch between components and the PCB and the new PCB laminates because they are more brittle than traditional PCB laminates.

Due to the anisotropy of tin grains and the fact that SnAgCu solder joints often consist of only one or a few tin grains, the number of tin grains in a solder joint and the orientation of them are crucial for the stress level in the solder joint, but also for the stress transferred to the PCB and BGA laminates. Since the orientation of the tin grains has a nearly random distribution, there may be a large difference in stress levels even for two neighbouring solder joints leading to that each solder joint to a BGA will have a unique stress condition. Thus, the solder joint with the highest stress level may be located randomly under the BGA, which may be far from the point of maximum shear stress for a BGA soldered with SnPb solder. Consequently, that can be expected to result in a high spread in failure distribution with some quite early failures.

As a result, it is important to clarify to what extent cracking has occurred in the PCB and BGA laminates in order to correctly interpret results from thermal cycling of area array components. The solder joints that are most prone to fatigue cracks are also the solder joints that are most likely to cause cracks in the laminate. Such cracks would moderate the stress on these solder joints causing a lower spread in failure distribution. The large spread in fatigue lives reported in the literature for similar BGA components indicates that laminate cracking may have affected the results in some of these investigations, but the laminate cracks have not been observed since they have not been looked for.

Another consequence of the test results is that for products that will be exposed to relatively large temperature variations in the field, for example automotive electronics, it may be necessary to avoid having a larger temperature range in the thermal cycling test than in the intended field environment. Otherwise, a wrong failure mechanism may be accelerated making the result invalid. That may necessitate testing times of one year or more. The impact of grain size and grain orientation in solder joints on laminate cracking must also be examined, quantified and understood when performing reliability simulations.

Acknowledgement

This work has performed with support from Swedish Governmental Agency for Innovation Systems (VINNOVA) within the FFI project “Lead-Free Electronics for Demanding Automotive Applications” (Grant Number 2010-02853).

References

1 Clech JP. Lead-Free Solder Joint Trends. In: Shangguan D, editor. Lead-free solder interconnect reliability, ASM International, 2005, pp. 107-28.
2 Mawer A, Levis K-M. Automotive PBGA assembly and board-level reliability with lead-free versus lead-tin interconnect. J SMT, Jan. 2001, pp. 9-16.
3 Smetana J, Coyle R, Sack T, Syed A, Love D, Tu D, Kummerl S. Pb-free solder joint reliability in a mildly accelerated test condition. In: Proc. IPC APEX EXPO, 2011.
4 Ma H, Lee T-K. Effects of board design variations on the reliability of lead-free solder joints. IEEE Trans Compon Packag Manuf Technol, Vol. 3, No. 1 2013, pp. 71-8. DOI: 10.1109/TCPMT.2012.2223214.
5 Willems G Vandevelde B. Impact of low CTE mold compounds on first- and second-level interconnect reliability. www.inemi.org/impact-low-cte-mold-compounds-first-and-second-level-interconnnect-reliability (last accessed June 2015).
6 Vandevelde B, Lofrano M, Willems G. Green mould compounds: Impact on second level interconnect reliability. In: Electronics Packaging Technology Conference, 2011. DOI: 10.1109/EPTC.2011.6184432.
7 Bieler TR, Jiang H, Lehman LP, Kirkpatrick T, Cotts EJ, Nandagopal B. Influence of Sn grain size and orientation on the thermomechanical response and reliability of Pb-free solder joints. IEEE Trans Compon Packag Technol, Vol. 31, Issue 2, 2008, pp. 370-81. DOI: 10.1109/TCAPT.2008.916835.
8 Bieler TR, Zhou B, Blair L, Zamiri A, Darbandi P, Pourboghrat F, Lee T-K, Liu K-C. The role of elastic and plastic anisotropy of Sn on microstructure and damage evolution in lead-free solder joints. In: Proc of the IEEE International Reliability Physics Symposium, 2011, pp. 5F.1.1-5F.1.9. DOI: 10.1109/IRPS.2011.5784538.
9 Barbini D, Meilunas M. Reliability of lead-free LGAs and BGAs: Effects of solder joint size, Cyclic Strain and Microstructure. In: Proc IPC APEX EXPO, 2013.
10 Mayyas A, Qasaimeh A, Borgesen P. Meilunas M. Effects of latent damage of crystallization on lead free solder joints. Microelectron Reliab, Vol. 54, 2014, pp. 447-56.
11 Bieler TR, Lee TK. Lead-free solder. In: Buschow JKH, Cahn RW, Flemings MC, Ilschner B, Kramer EJ, Mahajan S, Veyssière P (ed). Encyclopedia of Materials: Science and Technology, Elsevier, New York, 2010 pp 1–12.
12 Arfaei B, Anselm M, Mutuku F, Cotts E. A.R.E.A. – Effect of PCB surface finish on Sn grain morphology and thermal fatigue performance of lead-free solder joints. In: Proc SMTA Int, 2014.
13 Subramanian KN, Lee JG. Effect of anisotropy of tin on thermomechanical behavior of solder joints. J Materials Science: Materials in Electronics, Vol. 13, 2004, pp. 235-40. DOI: 10.1023/B:JMSE.0000012461.69417.75.
14 Zhou B. Characterization of tin crystal orientation evolution during thermal cycling in lead-free solder joints. Thesis, Michigan State University, 2012.
15 Erinc M, Assman TM, Schreurs PJG, Geers MGD. Fatigue fracture of SnAgCu solder joints by microstructural modeling. Int J of Fracture. Vol. 152, Issue 1, 2008, pp. 37-49. DOI: 10.1007/s10704-008-9264-9
16 Meilunas M, Primavera A, Dunford SO. Reliability and failure analysis of lead-free solder joints. In: Proc of the IPC Annual Meeting, 2002, paper S08-5.
17 Lehman LP, Kinyanjui RK, Wang J, Xing Y, Zavalij L, Borgesen P, Cotts EJ. Microstructure and damage evolution in Sn-Ag-Cu solder Joints. In: Proc Electronics Components and Technology Conference, Vol. 1, 2005, pp. 674-681.
18 Tegehall P-E, Dunn BD. Assessment of the reliability of solder joints to ball and column grid array packages for space applications. ESA STM-266, ESA Publications Division, Noordwijk, 2001.
19 Tegehall P-E, Dunn BD. Impact of cracking beneath solder pads in printed board laminate on reliability of solder joints to ceramic ball grid array packages. ESA STM-267, ESA Publications Division, Noordwijk, 2003.
20 Godbole G, Roggeman B, Borgesen P, Srihari K. On the nature of pad cratering. In: Proc Electronics Components and Technology Conference, 2009. DOI: 10.1109/ECTC.2009.5074003.
21 Xie D, Shangguan D, Kroener H. Pad cratering evaluation of PCB. In: Proc IPC APEX EXPO, 2006

22 Ma H, Ahmad M, Liu K-C. Acceleration factor study of lead-free solder joints under wide range thermal cycling conditions. In: Proc Electronics Components Technology Conference, 2010, pp. 1816-1822. DOI: 10.1109/ECTC.2010.5490719.
23 Raghavan V, Roggeman B, Meilunas M, Borgesen P. Effects of 'Latent Damage' on pad cratering: Reduction in life and a potential change in failure mode. Microelectron Reliab, 2013, Vol. 53, pp. 303-13. DOI:10.1016/j.microrel.2012.08.019.
24 Designing with high-density BGA packages for Altera Devices, Application Note 114, 2007. (last accessed Mar. 2015).
25 Darveaux R, Heckman J, Syed A, Mawer A. Solder joint fatigue life of fine pitch BGAs – Impact of design and material choices. Microelectron Reliab, Vol. 40, 2000, pp. 1117-1127. DOI: 10.1016/S0026-2714(00)00038-X.
26 Zhang J, Hai Z, Thirugnanasambandam S, Evans JF, Bozack MJ, Zhang Y, Suhling JC. Thermal aging effects on the thermal cycling reliability of lead-free fine pitch packages. IEEE. Trans Compon Packag Manuf. Technol, Vol. 3, No. 8, 2013, pp. 1348-57. DOI: 10.1109/TCPMT.2013.2251932.
27 Ghaffarian R, Nelson G, Cooper M, Lam D, Strudler S, Umdekar A, Selk K, Bjorndahl B, Duprey R. Thermal Cycling test results of CSP and RF package assemblies. In: Proc of Surface Mount International, 2000, pp. 850-7.
28 Kinyanjui R, Chu Q, Snugovski P, Coyle R. Solder joint reliability of Pb-free Sn-Ag-Cu ball grid array (BGA) components in Sn-Pb assembly process. In: Proc SMTA Int, 2007.
29 Lifanov I.I, Sherstyukov NG. Thermal expansion of copper in the temperature range -185 to +300°C. Measurement Techniques, Vol. 11, Issue 12, 1968, pp. 1653-9. DOI: 10.1007/BF00986433.
30 Ratanawilai TB, Hunter B, Subbarayan G, Rose D. A study on the variation of effective CTE of printed circuit boards through a validated comparison between strain gages and Moiré interferometry. IEEE Trans Compon Packag Technol, Vol. 26, No. 4, 2003, pp. 712-8. DOI: 10.1109/TCAPT.2003.821685.
31 Long G, Embree T, Mukadam M, Parupalli S, Vasudevan V. Lead free assembly impacts on laminate material properties and "pad crater" failures. In: Proc IPC APEX EXPO, 2007.
32 Raghavan V, Roggeman B, Meilunas M, Borgesen P. Effects of pre-stressing on solder joint failure by pad cratering. In: Proc Electronics Components Technology Conference, 2010, pp. 456-63. DOI: 10.1109/ECTC.2010.5490932.
33 Mukadam M, Long G, Butler P, Vasudevan V. Impact of cracking beneath solder pads in printed circuit boards on reliability of ball grid array packages. In: Proc SMTA Int, 2005.
34 Gray B, Eng P, McMahon J. Mechanical failures in Pb-free processing: Selected mitigation techniques for pad crater defects. In: Proc SMTA Int, 2011.
35 Hillman D, Wilcoxon R. JCAA/JG-PP lead-free solder testing for high reliability applications: -55°C to +125°C thermal cycle testing. SMTA J of Surface Mount Technology, Vol. 20, Issue 1, 2007, pp. 22-41.
36 Johansson J, Below I, Johnson E, Dudek R, Leisner P. Investigation on thermal fatigue of SnAgCu, Sn100C, and SnPbAg solder joints in varying temperature environments. Microelectron Reliab, Vol. 54, 2014, pp. 2523-35. DOI: 10.1016/j.microel.2014.06.007.
37 Smetana J, Coyle R, Read P. Koshmeider T, Love D, Kolenik M, Nguyen J. Thermal cycling reliability screening of multiple Pb-free solder ball alloys. In: Proc IPC APEX EXPO, 2010.